Available online at www.sciencedirect.com
SCIENCE DIRECT
Robotics and Autonomous Systems 54 (2006) 221–233
Robotics and Autonomous Systems
www.elsevier.com/locate/robot

Optimum design of the 5R symmetrical parallel manipulator with a surrounded and good-condition workspace

Xin-Jun Liu*, Jinsong Wang, Hao-Jun Zheng

Institute of Manufacturing Engineering, Department of Precision Instruments, Tsinghua University, Beijing, 100084, PR China

Received 4 November 2004; received in revised form 3 November 2005; accepted 9 November 2005
Available online 15 December 2005

Abstract

This paper concerns the optimum design issue of the 5R symmetrical parallel manipulator with a surrounded workspace. Generally, such a manipulator has a very large workspace. With different working modes, a manipulator will have different singular loci and workspaces. In this paper, the singularity and the *usable workspace* without singularity inside will be determined for the manipulator with a specified mode. The *usable workspace* can be used to define the global conditioning index (GCI). In order to obtain the optimum design of the manipulator, a non-dimensional design space is established. Because each of the non-dimensional manipulators in the established design space can represent the performances of all of its possible *similarity manipulators*, the design space is a very useful tool for guaranteeing a global comparative result. Within the design space, the singularity, *usable workspace* and control accuracy (evaluated using the GCI) are studied and the corresponding atlases are constructed. Based on the atlases, one can synthesize link lengths of the manipulator studied with respect to specified criteria. One example will be given to show how to use the atlases. In particular, an example will be presented of reaching the optimum dimensional result with respect to a desired practical workspace based on the optimum non-dimensional result identified from the atlases. For the reason that using the atlases presented in this paper a designer can obtain the optimum result with respect to any specification, the optimum design method proposed in this paper may be accepted by others.

Keywords: Parallel manipulator; Optimum design; Workspace; Conditioning index; Singularity

1. Introduction

Analysis and optimum design are two important issues in the development of a parallel manipulator. Without exhaustive analysis, a design will not be perfect or can even be lost. Then, analysis is primary. In the design process, kinematics and workspace are two typical problems because they are the basic model and reference for defining and evaluating the performances of a manipulator. For this reason, the kinematics and workspace are the most studied issues in the field [1–6]. The efforts were motivated by the fact that they would be finally applied in the design and application of the devices. Two issues are involved in the optimal design of a manipulator: performance evaluation and dimensional synthesis. Having designed a manipulator, it is necessary to evaluate its performances. A second problem is determining the dimensions (link lengths) of the manipulator, which is suitable for the task at hand. The latter is one of the most difficult issues in this field. In the optimum design process, several performance criteria could be involved for a design purpose, such as workspace [7–9], singularity [9], dexterity [10,11], accuracy [12], stiffness [13], and conditioning index [9].

The five-bar manipulator is a typical parallel manipulator with the minimal degrees of freedom (DoFs), which can be used for positioning a point on a region of a plane. A 5R parallel manipulator consists of five bars that are connected end to end by five revolute joints, two of which are connected to the base and actuated. Such a manipulator with a symmetric structure has attracted many researchers, who have investigated its position analysis [14], workspace [15,16], assembly modes [16,17], singularity [18,19], performance atlases [17] and kinematic design [19,20]. This paper concerns the 5R symmetrical parallel

* Corresponding author. Tel.: +86 1062796573; fax: +86 1062773375.
E-mail address: xinjunliu@mail.tsinghua.edu.cn (X.-J. Liu).

0921-8890/$ - see front matter © 2005 Elsevier B.V. All rights reserved.
doi:10.1016/j.robot.2005.11.002

manipulator with a surrounded workspace.[1] Generally, such a manipulator has a very large workspace.

The workspace of the 5R manipulator has been studied using different methods [15,16], e.g., geometric and numerical approaches, including a novel, simple and powerful method for numerically generating the workspace developed in [16]. But most of them are related to the theoretical workspace, which is the region consisting of inside singularity. Although the workspace of a manipulator with a specified forward configuration (the *up-configuration*) was presented in [16], there still exists singularity inside the workspace. A practical workspace is such a region without singularity, in which the manipulator should be controllable. As is well known, all global performance indices should be defined with respect to a workspace. In order to make the design more reasonable, it is necessary to present a workspace without singularity that can be used in the performance evaluation.

The singularity issue, especially singular loci, has been studied by other researchers [16,18,19]. But it has not been applied in the design of a 5R symmetric parallel manipulator yet. The reason for this is that the singularity was just shown in a general form. For example, all singular loci of the manipulator were illustrated in a chart developed in [19]. But, as we know, not all such singularities can occur for an assembled manipulator in practice. Because the manipulator cannot change its working mode from one to another, it is necessary to identify which singular loci the manipulator can have for a specified working mode.

In this paper, the singularity of the manipulator with a specified working mode is identified. The result helps us to define a useful workspace, which is the *usable workspace*. The workspace has no singularity inside and can be used to define a global index, e.g., the global conditioning index (GCI).

No matter how simple the 5R manipulator with a symmetrical structure is, the optimum design is always challenging. Many efforts have been contributed to this issue. For example, Gao et al. [15,17] developed a solution space trying to obtain the optimum design by means of atlases. The solution space is a good idea. However, because of unreasonable workspace presentation, the reported performance atlases cannot be applied to a practical design. Cervantes-Sánchez et al. [19] established a space made up of two normalized geometric parameters to show the characteristics of workspace and singularity. Because of its infinity, the tool cannot include all *similarity manipulators* in a finite space. Therefore, the space is not good enough for the optimum design. Besides this disadvantage, the workspace and singularity plotted in the space are in general forms, which are not those of a manipulator with specified inverse and forward kinematic modes. Then, they cannot be useful in the design. Other types of synthesis charts have been presented for the design of 5R manipulators in Refs. [21–23]. They may not yield manipulators that have certain desired benefits such as control accuracy and singularity-free workspace. Recently, the optimum design issue for the 5R symmetrical parallel manipulator was investigated in Ref. [20]. In that paper an optimum procedure was reported for obtaining the optimum results with respect to the ideal/isotropic condition number and bearing forces for force balancing. This methodology is a traditional one, implemented in MATLAB based on an established object function. It is good for providing an optimal result. However, it failed to illustrate the relationship between an index and the design parameters involved. The reader of the paper cannot know how optimal the result is. In addition, if the object function changes, a designer would have to start the optimization from the very beginning. For such reasons, the proposed procedures are difficult to accept as a unified methodology.

In order to study all possible 5R parallel manipulators with surrounded workspaces, in this paper, a design space is established according to the concept in [15,17,24]. The most important advantage of the design space is that each of the non-dimensional manipulators in the space can stand for all of its *similarity manipulators* in terms of performance. Any one of the dimensional 5R parallel manipulators can find its corresponding non-dimensional manipulator in the space. This fact is very important to us for comparing the performance of all manipulators. The comparative result can be illustrated by the performance atlas. In this paper, the atlases of singularity, *usable workspace* and GCI are plotted. Based on these atlases, an optimum region with respect to a large *usable workspace* and better GCI can be obtained. The region provides information on non-dimensional parameters of the manipulators. The candidate optimum results can be picked up from such a region. With respect to a desired practical workspace, the dimensional parameters of the optimum result can be obtained. Because of the advantage of the design space, the design method proposed in this paper can guarantee a global optimum result and can be developed as a unified method accepted by designers.

2. Kinematic problems

The 5R parallel manipulator, as shown in Fig. 1(a), is such a manipulator that the output point is connected to the base by two legs, each of which consists of three revolute joints and two links. The two legs are connected to a common point with the common revolute joint at the end of each leg. In each of the two legs, the revolute joint connected to the base is actuated. Such a manipulator can position a point freely in a plane.

A kinematics model of the manipulator is developed as shown in Fig. 1(b). Each actuated joint is denoted as A_i $(i = 1, 2)$, the other end of each actuated link is denoted as B_i and the common joint of the two legs is denoted as P, which is also the output point. A fixed global reference system O–xy is located at the center of A_1A_2 with the y axis normal to A_1A_2 and the x axis directed along A_1A_2. For the structure symmetry, we have $OA_1 = OA_2$, $A_1B_1 = A_2B_2$ and $B_1P = B_2P$. The length of the actuated link for each leg is denoted as $A_iB_i = R_1(r_1)$. Additionally, $B_iP = R_2(r_2)$ and $OA_i = R_3(r_3)$. Here, R_j $(j = 1, 2, 3)$ are link lengths with dimension and r_j $(j = 1, 2, 3)$ are those without dimension.

[1] A manipulator with a surrounded workspace is defined as the manipulator whose base joints are bordered around with workspace points.

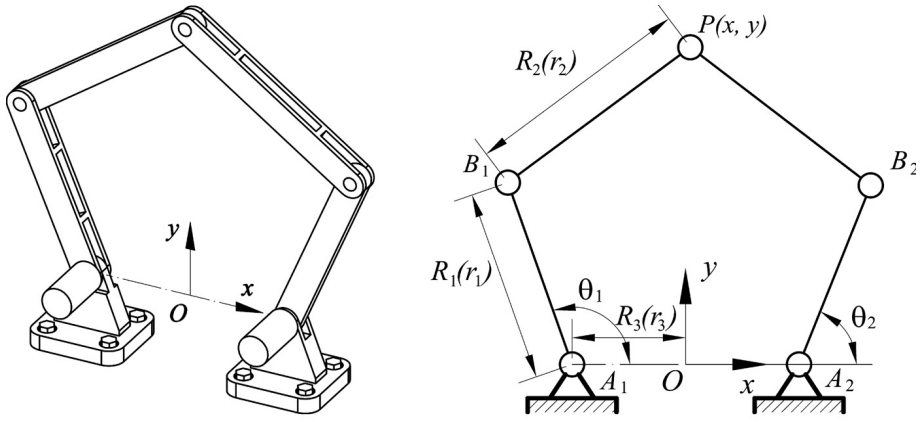

(a) (b)

Fig. 1. The 5R parallel manipulator.

2.1. Inverse kinematics

The position of the output point P in the reference system O–xy can be described by the position vector $\boldsymbol{p}$, and we have

$$\boldsymbol{p} = \begin{pmatrix} x & y \end{pmatrix}^{\mathrm{T}}. \tag{1}$$

In the reference frame O–xy, the position vectors $\boldsymbol{b}_i$ of points B_i can be written as

$$\begin{aligned} \boldsymbol{b}_1 &= \begin{pmatrix} r_1\cos\theta_1 - r_3 & r_1\sin\theta_1 \end{pmatrix}^{\mathrm{T}} \quad \text{and} \\ \boldsymbol{b}_2 &= \begin{pmatrix} r_1\cos\theta_2 + r_3 & r_1\sin\theta_2 \end{pmatrix}^{\mathrm{T}} \end{aligned} \tag{2}$$

where θ_1 and θ_2 are the input angles of the two legs. Then, the inverse kinematic problem can be solved by writing following constraint equation

$$|\boldsymbol{pb}_i| = r_2, \qquad i = 1, 2 \tag{3}$$

in another form

$$(x - r_1\cos\theta_1 + r_3)^2 + (y - r_1\sin\theta_1)^2 = r_2^2 \tag{4}$$

$$(x - r_1\cos\theta_2 - r_3)^2 + (y - r_1\sin\theta_2)^2 = r_2^2 \tag{5}$$

from which, if the position of output point P is known, the inputs for reaching the position can be obtained as

$$\theta_i = 2\tan^{-1}(z_i), \qquad i = 1, 2 \tag{6}$$

where

$$z_i = \frac{-b_i \pm \sqrt{b_i^2 - 4a_i c_i}}{2a_i}, \qquad i = 1, 2 \tag{7}$$

in which

$$\begin{aligned} a_1 &= r_1^2 + y^2 + (x + r_3)^2 - r_2^2 + 2(x + r_3)r_1 \\ b_1 &= -4yr_1 \\ c_1 &= r_1^2 + y^2 + (x + r_3)^2 - r_2^2 - 2(x + r_3)r_1 \\ a_2 &= r_1^2 + y^2 + (x - r_3)^2 - r_2^2 + 2(x - r_3)r_1 \\ b_2 &= b_1 = -4yr_1 \\ c_2 &= r_1^2 + y^2 + (x - r_3)^2 - r_2^2 - 2(x - r_3)r_1. \end{aligned}$$

From Eq. (7), one can see that there are four solutions for the inverse kinematic problem of the 5R manipulator. The configuration shown in Fig. 1 can be obtained if the sign "±" in Eq. (7) is "+" for the case $i = 1$ and is "−" for $i = 2$. Such a configuration is denoted as the "+−" model. Then there are three others, which are "−+", "−−", and "++" models, respectively. These four inverse kinematics models correspond to four types of working modes.

2.2. Forward kinematics

The forward kinematic problem is obtaining the output with respect to a set of given inputs. From Eqs. (4) and (5), one obtains

$$\begin{aligned} &x^2 + y^2 - 2(r_1\cos\theta_1 - r_3)x - 2r_1\sin\theta_1 y \\ &\quad - 2r_1r_3\cos\theta_1 + r_3^2 + r_1^2 - r_2^2 = 0 \end{aligned} \tag{8}$$

$$\begin{aligned} &x^2 + y^2 - 2(r_1\cos\theta_2 + r_3)x - 2r_1\sin\theta_2 y \\ &\quad + 2r_1r_3\cos\theta_2 + r_3^2 + r_1^2 - r_2^2 = 0. \end{aligned} \tag{9}$$

Eqs. (8) and (9) yield

$$x = ey + f \tag{10}$$

in which

$$e = \frac{r_1(\sin\theta_1 - \sin\theta_2)}{2r_3 + r_1\cos\theta_2 - r_1\cos\theta_1}$$

and

$$f = \frac{r_1r_3(\cos\theta_2 + \cos\theta_1)}{2r_3 + r_1\cos\theta_2 - r_1\cos\theta_1}.$$

Substituting Eq. (10) into Eq. (8) yields

$$dy^2 + gy + h = 0 \tag{11}$$

where

$$\begin{aligned} d &= 1 + e^2 \\ g &= 2(ef - er_1\cos\theta_1 + er_3 - r_1\sin\theta_1) \\ h &= f^2 - 2f(r_1\cos\theta_1 - r_3) - 2r_1r_3\cos\theta_1 + r_3^2 + r_1^2 - r_2^2. \end{aligned}$$

Then, y can be obtained from Eq. (11) as

$$y = \frac{-g \pm \sqrt{g^2 - 4dh}}{2d}. \tag{12}$$

From Eqs. (10) and (12), one sees that there are two solutions for the forward kinematic problem of the manipulator. They correspond to two types of assembly modes. The corresponding configurations are called the *up-* and *down-configurations*. The *up-configuration* can be reached when the sign "±" in Eq. (12) is "+".

In this paper, we are concerned about the manipulator with the "+−" model and, at the same time, the *up-configuration*.

3. Jacobian matrix

Eqs. (4) and (5) can be differentiated with respect to time to obtain the velocity equations, which leads to

$$\begin{aligned} &r_1 [y\cos\theta_1 - (x + r_3)\sin\theta_1]\,\dot{\theta}_1 \\ &\quad = (x + r_3 - r_1\cos\theta_1)\,\dot{x} + (y - r_1\sin\theta_1)\,\dot{y} \end{aligned} \tag{13}$$

$$\begin{aligned} &r_1 [y\cos\theta_2 + (r_3 - x)\sin\theta_2]\,\dot{\theta}_2 \\ &\quad = (x - r_3 - r_1\cos\theta_2)\,\dot{x} + (y - r_1\sin\theta_2)\,\dot{y}. \end{aligned} \tag{14}$$

Rearranging Eqs. (13) and (14) leads to an equation of the form

$$\boldsymbol{A}\dot{\boldsymbol{\theta}} = \boldsymbol{B}\dot{\boldsymbol{p}} \tag{15}$$

where $\dot{\boldsymbol{p}}$ is the vector of output velocities defined as

$$\dot{\boldsymbol{p}} = \begin{pmatrix} \dot{x} & \dot{y} \end{pmatrix}^{\mathrm{T}} \tag{16}$$

and $\dot{\boldsymbol{\theta}}$ is the vector of input velocities defined as

$$\dot{\boldsymbol{\theta}} = \begin{pmatrix} \dot{\theta}_1 & \dot{\theta}_2 \end{pmatrix}^{\mathrm{T}}. \tag{17}$$

Matrices $\boldsymbol{A}$ and $\boldsymbol{B}$ are, respectively, the 2×2 matrices of the manipulator and can be expressed as

$$\boldsymbol{A} = \begin{bmatrix} y\cos\theta_1 - (x + r_3)\sin\theta_1 & 0 \\ 0 & y\cos\theta_2 + (r_3 - x)\sin\theta_2 \end{bmatrix} r_1 \tag{18}$$

$$\boldsymbol{B} = \begin{bmatrix} x + r_3 - r_1\cos\theta_1 & y - r_1\sin\theta_1 \\ x - r_3 - r_1\cos\theta_2 & y - r_1\sin\theta_2 \end{bmatrix}. \tag{19}$$

The Jacobian matrix of the manipulator can be written as

$$\boldsymbol{J} = \boldsymbol{A}^{-1}\boldsymbol{B}. \tag{20}$$

4. Singularity analysis

The singularity of the 5R symmetrical parallel manipulator has been studied by many researchers. Here, we summarize this issue as follows.

(1) The first kind of singularity occurs when $\boldsymbol{A}$ becomes singular but $\boldsymbol{B}$ remains invertible. Physically, this corresponds to the configuration whenever one of the legs A_1B_1P and A_2B_2P is completely extended or folded. From the analysis of the workspace, this singularity occurs when the output point P reaches its limit or is at the boundary of the workspace. This singularity is also called *serial singularity*. The loci of this kind of singularity are actually given by the following circles

$$C_{1o} : (x + r_3)^2 + y^2 = (r_1 + r_2)^2 \tag{21}$$

$$C_{1i} : (x + r_3)^2 + y^2 = (r_1 - r_2)^2 \tag{22}$$

$$C_{2o} : (x - r_3)^2 + y^2 = (r_1 + r_2)^2 \tag{23}$$

$$C_{2i} : (x - r_3)^2 + y^2 = (r_1 - r_2)^2. \tag{24}$$

Note that $r_1 = 0$ leads to $\det(\boldsymbol{A}) = 0$ as well. But this also leads to an unmovable manipulator.

(2) The second kind of singularity, occurring only in closed kinematics chains, arises when $\boldsymbol{B}$ becomes singular but $\boldsymbol{A}$ remains invertible. Usually, there are two cases for this singularity. The first case is that B_1PB_2 is completely folded, i.e., the points B_1 and B_2 are coincident. When this condition occurs the locus of the point P can be described by

$$\begin{aligned} &x^2 + \left(y - \sqrt{r_1^2 - r_3^2}\right)^2 = r_2^2 \qquad \text{or} \\ &x^2 + \left(y + \sqrt{r_1^2 - r_3^2}\right)^2 = r_2^2. \end{aligned} \tag{25}$$

Please note that, if $r_3 = 0$, this type of singularity can occur easily when links A_1B_1 and A_2B_2 are coincident. For this case, the loci of point P is an annulus, which is bounded by two circles

$$x^2 + y^2 = (r_1 + r_2)^2 \quad \text{and} \quad x^2 + y^2 = (r_1 - r_2)^2. \tag{26}$$

The second case is that when B_1PB_2 is completely extended. The locus of point P for this type of singularity can be described by

$$\begin{cases} x = r_1(\cos\theta_2 + \cos\theta_1)/2 \\ y = r_1(\sin\theta_2 + \sin\theta_1)/2 \end{cases} \tag{27}$$

where

$$\begin{aligned} &\theta_1 \in [0, 2\pi] \\ &\theta_2 = 2\tan^{-1}(z) \\ &z = (-b \pm \sqrt{b^2 - 4ac})/(2a) \\ &a = 4r_2^2 + 4r_1r_3\cos\theta_1 + 4r_1r_3 - 4r_3^2 - 2r_1^2 - 2r_1^2\cos\theta_1 \\ &b = 4r_1^2\sin\theta_1 \\ &a = 4r_2^2 + 4r_1r_3\cos\theta_1 - 4r_1r_3 - 4r_3^2 - 2r_1^2 + 2r_1^2\cos\theta_1. \end{aligned}$$

For the second kind of singularity, if $r_1 < r_3$, the singularity where B_1 and B_2 are coincident will not occur. If $r_2 > r_1 + r_3$, there is no singularity where B_1PB_2 is completely extended.

(3) The third kind of singularity occurs when both $\boldsymbol{A}$ and $\boldsymbol{B}$ become simultaneously singular. This singularity is of a slightly different nature than the first two since it is not only configuration but also architecture dependent.

From the analysis of the first and second kinds of singularities, one can see that the third kind of singularity occurs when the five points A_1, B_1, P, B_2 and A_2 are collinear.

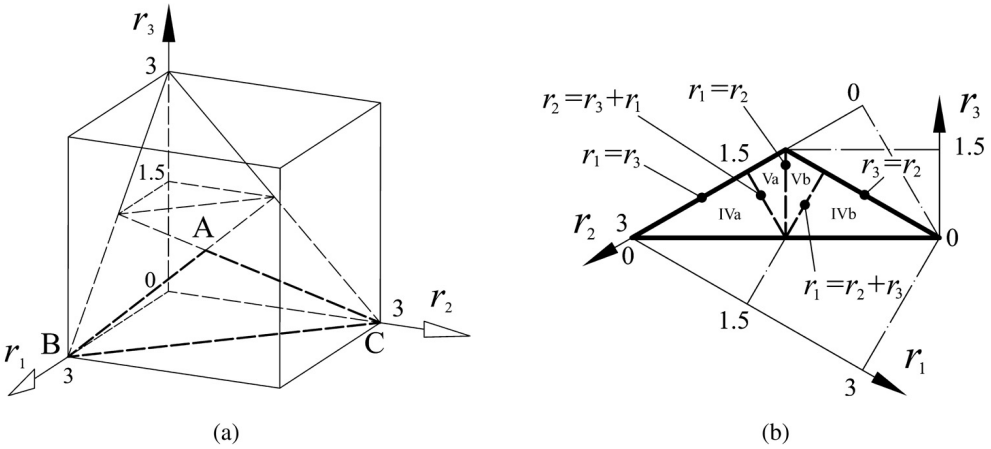

Fig. 2. Design space of the 5R parallel manipulator with a surrounded workspace.

There are six cases for this kind of singularity. The parameter conditions for those singularities are:

(a) $r_1 = r_3$;
(b) $r_2 = r_3$;
(c) $r_3 = r_1 + r_2$;
(d) $r_2 = r_1 + r_3$;
(e) $r_1 = r_3 + r_2$;
(f) $r_3 = 0$.

A manipulator that satisfies any one of the five parameter conditions (a)–(e) is called *a change point manipulator*.

5. The design space of the 5R parallel manipulator

As is well known, the performance of a parallel manipulator depends on not only the pose of the moving platform but also link lengths (dimensions). Disregarding the pose, each of the links can be the length between zero and infinity. There are always several links in a parallel manipulator. Then the combination of the links with different lengths will be infinite. They undoubtedly have different performance characteristics. To apply a specified manipulator in practice, we usually should determine its link lengths with respect to a desired application. This is actually the so-called optimum design (parameter synthesis) of a manipulator. In this process, one of the most classical tools that has been used is the chart, which can show the relationship between performances and link lengths. To make it work, we should first establish a space that contains all links involved. Next is plotting the chart considering a desired performance. In this paper, the space is called *the design space*. The chart that can show the relationship between performances and link lengths is called the *atlas*. The *index* is used to evaluate a performance. Normally, several indices will be considered in the design process.

For the parallel manipulator considered here, because of the symmetric structure there are three parameters, which are R_1, R_2 and R_3 as shown in Fig. 1. Any one of the parameters R_1, R_2 and R_3 can take any value between zero and infinity. This is the big problem for building up a design space that can embody all manipulators (with different link lengths) in a finite space. For this reason, we must eliminate the physical link size of the manipulators. Let

$$D = (R_1 + R_2 + R_3)/3. \tag{28}$$

One can obtain three non-dimensional parameters r_i by means of

$$r_1 = R_1/D, \qquad r_2 = R_2/D, \qquad r_3 = R_3/D. \tag{29}$$

Then we have

$$r_1 + r_2 + r_3 = 3. \tag{30}$$

Theoretically, from Eq. (30), the three non-dimensional parameters r_1, r_2 and r_3 can take any value between 0 and 3. For the 5R parallel manipulator studied here, the analysis on the workspace and singularity shows that r_1 and r_2 cannot be 0 and $r_1 + r_2$ cannot be less than r_3, otherwise they will result in the failure of manipulator assembly. Therefore, the three parameters should be

$$0 < r_1, \quad r_2 < 3 \quad \text{and} \quad 0 \le r_3 \le 1.5. \tag{31}$$

Here, we are concerned with the manipulator with a surrounded workspace. Such a manipulator is defined as the manipulator whose base joints A_i ($i = 1, 2$) are bordered around with workspace points. For such a manipulator, both of the actuated links must at least be cranks. The parameter condition for such a manipulator is:

$$|r_1 - r_2| \le r_1 + r_2 - 2r_3, \quad \text{i.e., } r_2 \ge r_3 \quad \text{and} \quad r_1 \ge r_3. \tag{32}$$

Based on Eqs. (30)–(32), one can establish a design space as shown in Fig. 2(a), in which the isosceles triangle ABC is actually the design space. In Fig. 2(a), the triangle ABC is restricted by r_1, r_2 and r_3. Therefore it can be figured in another form as shown in Fig. 2(b), which is called the planar-closed configuration of the design space. Comparing Fig. 2(a) with (b), one can see that the trapezoid ABC in Fig. 2(b) is slightly different from that in Fig. 2(a). But both of them are restricted

by Eqs. (30)–(32). Fig. 2(b) will be more convenient for us for plotting an atlas.

In order to study the performance of the parallel manipulator in detail, three lines $r_2 = r_1 + r_3$, $r_1 = r_3 + r_2$ and $r_1 = r_2$ can be used to divide the design space into four sub-regions, i.e., IVa, IVb, Va and Vb, as shown in Fig. 2(b). Such a design space will help us to investigate in detail the performance characteristics of all 5R parallel manipulators with possible combinations of $R_1(r_1)$, $R_2(r_2)$ and $R_3(r_3)$.

We would like to mention that the concept using non-dimensional parameters to establish a finite space of a parallel manipulator was introduced in [15,17,24], where the space is called *the physical model of the solution space*, which was used to study some performances of the 5R parallel manipulator in [15,17]. The performances were based on the theoretical workspace without the consideration of singularity. For example, according to the result in [17], the atlas of the global conditioning index for the manipulator with the working mode "+−" is the same as that of the manipulator with the "−+" mode. But the analysis in this paper will show that the singular loci and workspace without singularity will be different for different working modes. For this reason, practically, the atlases obtained in the references cannot be used directly by readers. In this paper, the singularity will be taken into account throughout the evaluation of the performances and the optimum design of the parallel manipulator. Therefore, the result of the paper will be more precise and can be referred to by others.

6. Distribution characteristics of singular loci in the design space

Based on the analysis on the singularity, there exist two kinds of singular loci. The first one is the first kind of singular locus. The loci are C_{1o}, C_{1i}, C_{2o} and C_{2i} given by Eqs. (21)–(24), respectively. They are actually the boundaries of the theoretical workspace. The second one is the second kind of singular locus. There are two cases for this kind of singular locus. One is that when the points B_1 and B_2 are coincident. The loci are actually two circles given by Eq. (25), which are denoted as $C_{\text{Coin-}U}$ and $C_{\text{Coin-}D}$, respectively. The second case occurs when B_1PB_2 is completely extended. The locus is represented by Eq. (27), which is denoted as C_{Col}.

For example, for the manipulator with $r_1 = 1.2$, $r_2 = 1.0$ and $r_3 = 0.8$, the singular loci are shown in Fig. 3.

The singular loci for different manipulators will be different. They can be illustrated by Fig. 4, from which one can see that

- For a specified manipulator, the distribution of singular loci within the workspace is symmetric about the x and y axes.
- The distribution in the design space is not symmetric with respect to $r_1 = r_2$.
- For the manipulators in sub-region IVa where $r_1 + r_3 < r_2$, there is no singular locus C_{Col} in their workspaces. For these manipulators, B_1PB_2 cannot be completely extended.

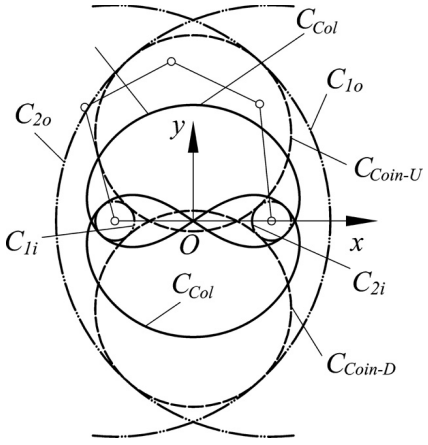

Fig. 3. Singular Loci of a manipulator.

7. The usable workspace

7.1. Definition

Because there exist singular loci inside the theoretical workspace, if a manipulator wants to move from one point to another it maybe should pass a singular configuration. That means it should change from one working mode to another. In practice, changing working mode during the working process is definitely impossible. Therefore, we should find a working space without singularity.

The *usable workspace* is defined as the maximum continuous workspace that contains no singular loci inside but is bounded by singular loci outside. According to this definition, not every point within the *usable workspace* can be available for a practical manipulator. The manipulator will be out of control at the points on the boundaries and in their neighborhoods. But within this region, the manipulator with a specified working mode can move freely.

In Section 6, the first and second kinds of singular loci have been presented for the manipulator in each sub-region as shown in Fig. 4. The first kind of singularity is actually the boundary of a theoretical workspace. Then, a manipulator with every working mode has such singular loci. However, because the second kind of singularity occurs inside the workspace, not every working mode has all such singularities. Normally, there are tangent points between the first and second kinds of singular loci. At these points, the manipulator is in the configurations that change the working modes. The points can be used to identify which singular loci a specified mode has. It is noteworthy that, for the manipulators in the sub-region IVb where $r_1 > r_2 + r_3$ and $r_2 > r_3$, the parameter condition does not allow the case where the singular locus C_{Col} and the first kind of singular locus are tangent to occur. These manipulators with the working modes "++" and "−−" have no singularity where B_1PB_2 is completely extended.

In this paper, we are concerned about the manipulator with both the working mode "+−"and the *up-configuration*, simultaneously. Fig. 5 shows the singular loci for the manipulators in the design space.

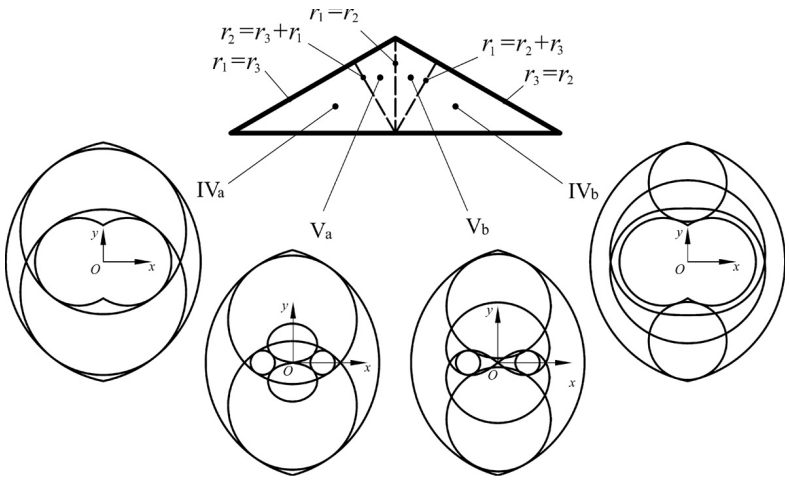

Fig. 4. Distribution of singular loci in the design space.

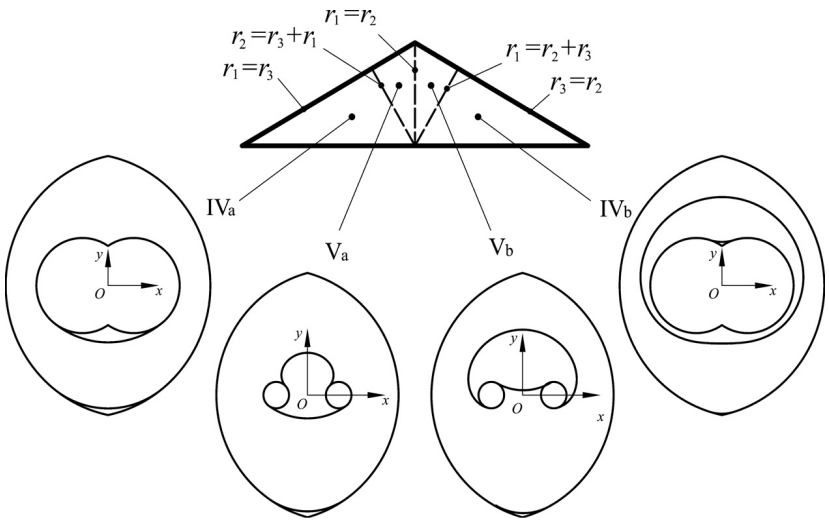

Fig. 5. Distribution of singular loci in the design space for the manipulator with the working mode "+−".

The singular loci shown in Fig. 5 can be used to determine the *usable workspace* of a 5R parallel manipulator with both the working mode "+−" and the *up-configuration*. For example, the *usable workspace* of the manipulator with $r_1 = 1.2$, $r_2 = 1.0$ and $r_3 = 0.8$ is shown as the hatched region in Fig. 6. Within this workspace, the manipulator has the configuration with both the working mode "+−" and the *up-configuration*.

7.2. Distribution of the usable workspace shape in the design space

The *usable workspace* shape for the 5R parallel manipulator can be classified in the design space as shown in Fig. 7, where each of the shaded regions is the *usable workspace* of the manipulator with the "+−" working mode and the *up-configuration*, simultaneously. From the distribution one sees that each *usable workspace* is symmetric about the y axis.

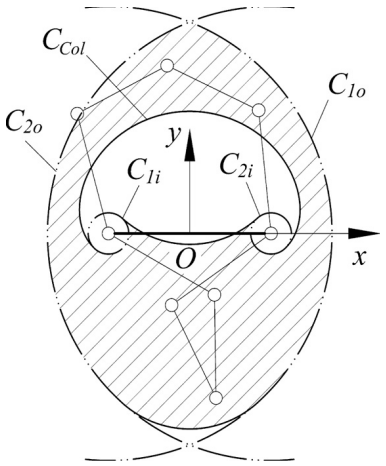

Fig. 6. *Usable workspace* of a manipulator.

7.3. Atlas of the usable workspace area

Using the numerical method, the *usable workspace* area can be calculated for every manipulator. The atlas can be plotted in the design space as shown in Fig. 8, from which one can see that when r_1 is specified the workspace area is inversely proportional to r_3.

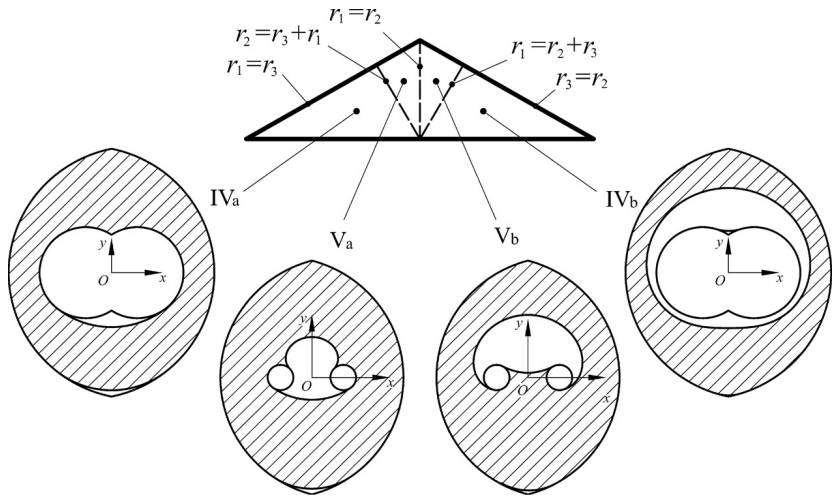

Fig. 7. *Usable workspace* shape in the design space.

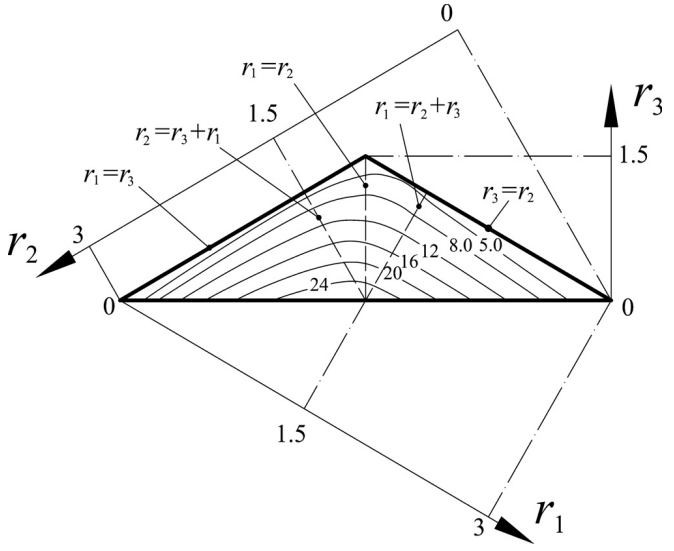

Fig. 8. Atlas of the *usable workspace* area.

From Figs. 7 and 8, one can completely know the workspace performance of any 5R parallel manipulator with non-dimensional parameters r_1, r_2 and r_3.

8. Global conditioning index and its atlas

Mathematically, the condition number of a matrix is used in numerical analysis to estimate the error generated in the solution of a linear system of equations by the error on the data [25]. When applied to the Jacobian matrix, the condition number will give a measure of the accuracy of the control of the manipulator [26]. It can be also used to evaluate the dexterity and isotropy of a manipulator [9,10,27–29]. This number must be kept as small as possible. If the number can be unity, the matrix is an isotropic one, and the manipulator is in an isotropic configuration.

The condition number κ_J is configuration-dependent. Its reciprocal $1/\kappa_J$ $(0 < 1/\kappa_J \leq 1)$ is a local performance index that is called *local conditioning index* (LCI). In order to evaluate the global behavior of a manipulator on a workspace, a global index can be defined as [30]

$$\eta_J = \frac{\int_W \frac{1}{\kappa_J} \mathrm{d}W}{\int_W \mathrm{d}W} \tag{33}$$

which is the *global conditioning index* (GCI). In Eq. (33), W is the *usable workspace* of the manipulator. In particular, a large value of the index ensures that the manipulator can be precisely controlled.

The atlas of the GCI for the manipulator is shown in Fig. 9, from which one can see that:

- If r_1 is specified the GCI value is inversely proportional to r_3.
- The manipulator with best GCI is in the sub-region IVa.

9. Optimum design example based on atlases

9.1. Optimum region with respect to workspace and GCI

Relationships between performances, such as workspace and GCI, and link lengths of the 5R symmetrical parallel manipulator with a surrounded workspace have been studied in the earlier sections. The results have been illustrated by their atlases, from which one can visually know which manipulator can have a better performance and which cannot. This is very important to us for finding a global optimum manipulator for a specified application.

In most designs, the workspace and GCI are usually considered. From the atlas of *usable workspace* area (Fig. 8), we can see that the smaller the parameter r_3 the larger the *usable workspace*. From the atlas of GCI (Fig. 9), we know that the manipulator with better GCI is in the sub-region IVa. If the *usable workspace* area is supposed to be greater than 24.0 and the GCI greater than 0.7, an optimum region in the design space can be obtained as shown in Fig. 10. The region is denoted as Ω_{W-GCI}, which is restricted by three non-dimensional parameters with $1.16 \leq r_1 \leq 1.40$, $1.543 \leq r_2 \leq 1.80$ and $0.0 \leq r_3 \leq 0.131$.

After the optimum region is obtained, there are two ways to reach the optimum design result with non-dimensional

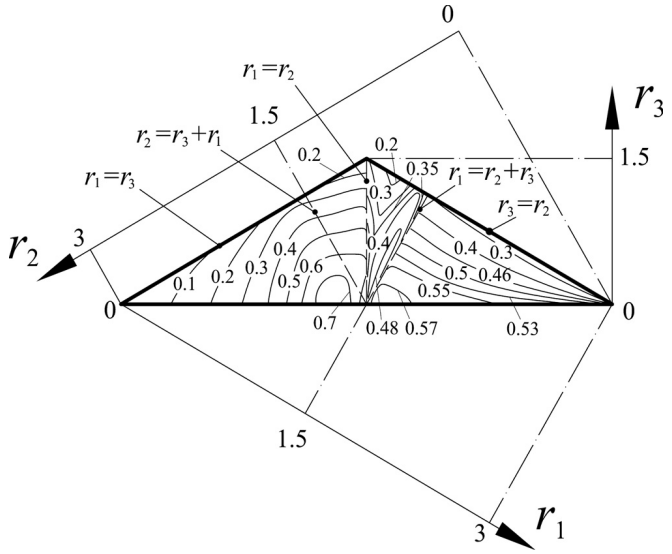

Fig. 9. The atlas of the global conditioning index.

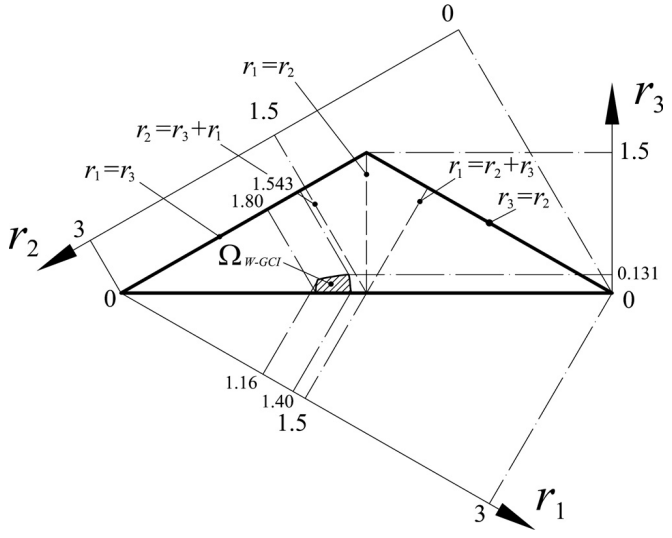

Fig. 10. One optimum region with specified *usable workspace* area and GCI.

parameters. One is to search for a most optimal result within the region Ω_{W-GCI} using one classical searching algorithm based on an established object function. This is not within the scope of this paper. Another one is to select a manipulator within the optimum region obtained. For example, the manipulator with $r_1 = 1.3, r_2 = 1.6$ and $r_3 = 0.1$ can be selected as the candidate if only workspace and GCI are involved in the design. Its *usable workspace* area is 24.67 and the GCI value 0.7482. Because $r_2 > r_1 + r_3$ and $r_1 > r_3$, the manipulator is in the sub-region IVa. There is no the singularity where B_1PB_2 is completely extended in its workspace. The workspace is shown in Fig. 11.

Notably, the example is not the most optimal manipulator with respect to the workspace and GCI performances. The optimum region is undoubtedly not suitable for all design conditions. We could not predict all design specifications previously. Ω_{W-GCI} is just one example to show how to get

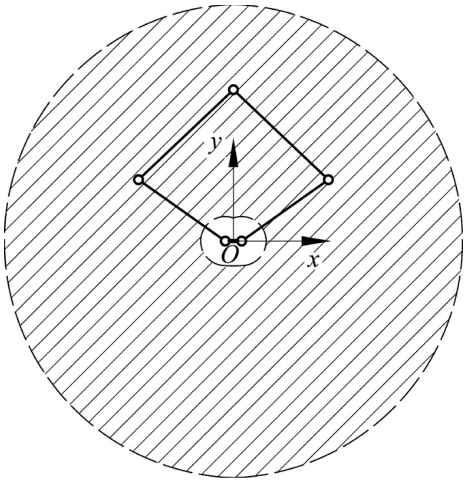

Fig. 11. One example in the optimum region Ω_{W-GCI}.

an optimum region. From Figs. 8 and 9, one can see that the manipulator with very large *usable workspace* and best GCI should be that with $r_3 = 0.0$. One example is that with $r_1 = 1.28, r_2 = 1.72$ and $r_3 = 0.0$. Its *usable workspace* area is 27.67 and the GCI value 0.8093. There is also no singularity inside its workspace. The manipulator and its workspace are shown in Fig. 12.

9.2. Dimension determination of the optimum manipulator with respect to a practical workspace

In the design space, parameters r_1, r_2 and r_3 have no dimension. They are the ratios of the dimensional parameters R_j $(j = 1, 2, 3)$ to a dimensional scale D. As given in Eqs. (31) and (32), parameters r_1, r_2 and r_3 are limited. But each of the parameters R_1, R_2 and R_3 can be infinite. Practically, we are concerned about the dimensional manipulator but not the non-dimensional one. It is not difficult to find that the ratio $R_1{:}R_2{:}R_3$ is always equal to $r_1{:}r_2{:}r_3$. For any possible dimension combination of R_1, R_2 and R_3, one can always find its corresponding group of r_1, r_2 and r_3 in the design space.

In the last section, one optimum region considering the workspace and GCI performances is obtained in the design space. The optimum region is restricted by three non-dimensional parameters r_1, r_2 and r_3. Two manipulator examples in the optimum region are presented. As an example of presenting how to determine the real dimensional parameters based on a non-dimensional optimum manipulator, we consider the manipulator with $r_1 = 1.28, r_2 = 1.72$ and $r_3 = 0.0$ shown in Fig. 12.

The process for finding dimensions of the non-dimensional optimum manipulator with respect to a desired practical workspace can be summarized as follows:

Step 1: To obtain the *good-condition workspace* with a specified LCI. According to the definition of *usable workspace* in Section 7.1, a *usable workspace* is not the space that can be used in practice by a manipulator. Actually, only part of the *usable workspace* can be available for a device. Here,

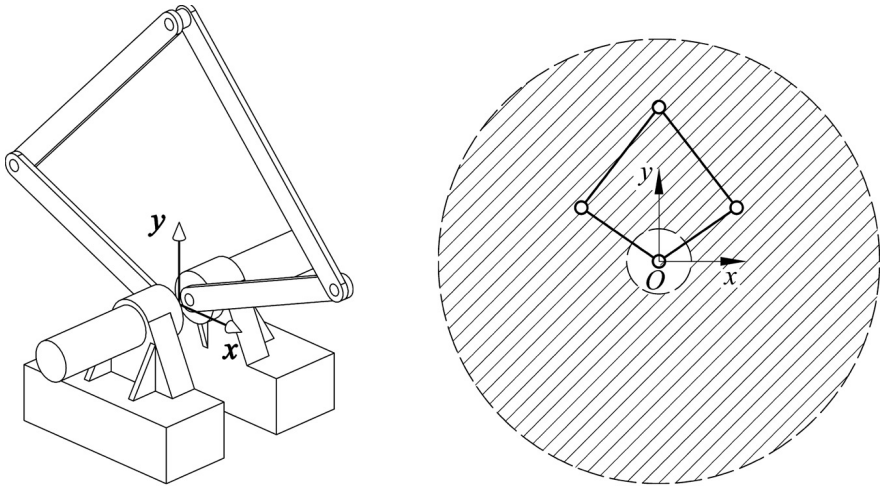

Fig. 12. One optimum example with large *usable workspace* and best GCI: (a) 3D model of the manipulator; (b) the *usable workspace*.

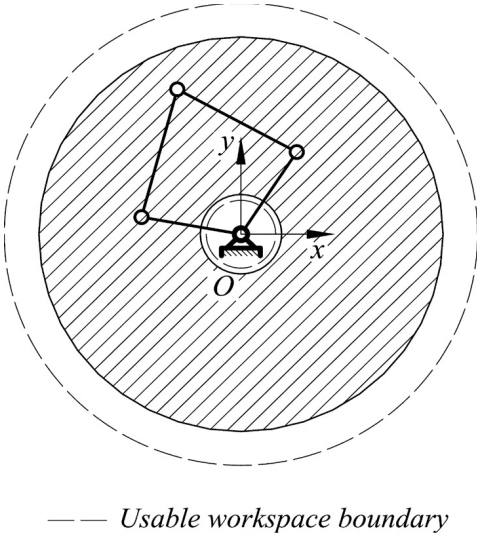

Fig. 13. The *good-condition workspace* with $1/\kappa_J \geq 0.5$ for the non-dimensional optimum example.

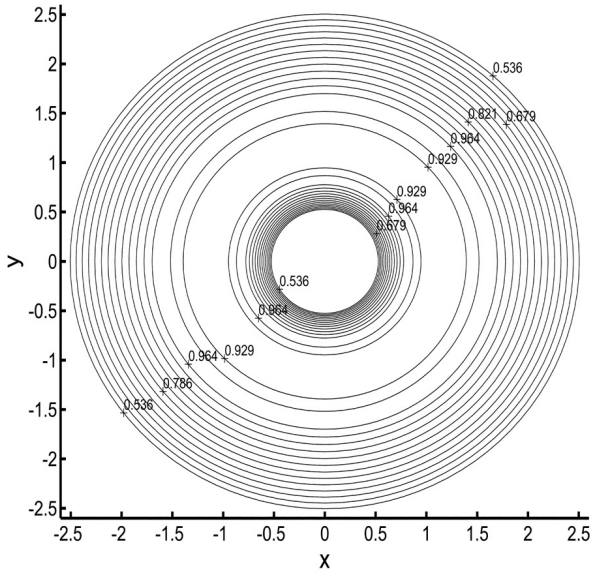

Fig. 14. Distribution of LCI on the *good-condition workspace* of the non-dimensional optimum example.

the available region is referred to as the *practical workspace* or *good-condition workspace*, which can be restricted by the LCI. The index value can be determined by the designer. For example, if the LCI is given as $1/\kappa_J = 0.5$, the *good-condition workspace* of the manipulator with $r_1 = 1.28$, $r_2 = 1.72$ and $r_3 = 0.0$ is shown in Fig. 13. It is bounded by two circles with radii 0.5154 and 2.5614. The workspace area is 19.78. The GCI index within this workspace is $\eta_J = 0.8502$. Fig. 14 shows the distribution of LCI on this workspace.

Step 2: To determine the dimensional factor D, which was used to change the dimensional geometric parameters of a manipulator to those with no dimension. The ratio of the workspace W_{Dim} of a dimensional manipulator to that $W_{\text{Non-Dim}}$ of a non-dimensional manipulator is D^2, that is

$$W_{\text{Dim}} = D^2 W_{\text{Non-Dim}}. \tag{34}$$

This relationship is not difficult to find by comparing the workspaces of the manipulator with R_1, R_2 and R_3 and that with r_1, r_2 and r_3. The *good-condition workspace* of the non-dimensional optimum manipulator is obtained in Step 1. If the workspace of a dimensional manipulator is given with respect to the design specification, the factor D can be reached from Eq. (34) easily. For example, if the objective workspace is identical with the *good-condition workspace* shown in Fig. 13 in shape and the workspace area is 400 mm^2, the factor D can be obtained as $D = \sqrt{400/19.78} \approx 4.5$ mm. Notably, the desired workspace can be any shape. But the shrunken workspace about D must be embodied in the *good-condition workspace*.

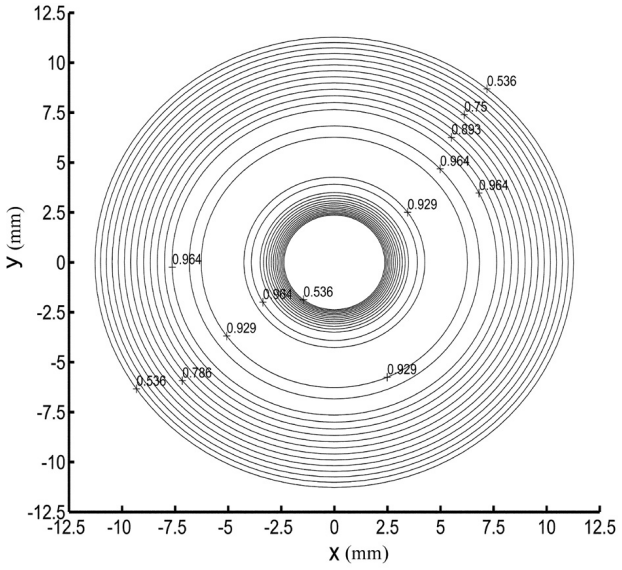

Fig. 15. Distribution of LCI on the dimensional workspace.

Step 3: To reach the dimensional parameters of the optimum manipulator by means of the dimensional factor D. As given in Eq. (29), the relationship between a dimensional parameter and a non-dimensional one is $R_j = Dr_j$ ($j = 1, 2, 3$). Then, if D is determined, R_j can be reached. For the above example, we have $R_1 = 5.76$ mm, $R_2 = 7.74$ mm and $R_3 = 0.0$ mm. In this step, one can also check the performances of the dimensional manipulator. For example, Fig. 15 shows the distribution of LCI on the dimension workspace. From this one can see that the distribution is the same as that shown in Fig. 14 of the non-dimensional manipulator. The GCI is still equal to 0.8502. Then, the factor D does not change the conditioning index and the distribution on the workspace.

Step 4: To calculate the input limit for θ_1 and θ_2. The inputs can be calculated from the inverse kinematic equation. Because the manipulator studied here has a surrounded workspace, the limit for each of θ_1 and θ_2 is undoubtedly $[0, 360°]$.

From this section, one can see that all manipulators with parameters $R_j = Dr_j$ ($j = 1, 2, 3$) have similar performances to that with the non-dimensional parameters r_j. For example, the workspace of the manipulator with R_j is D^2 times that of the manipulator with r_j. These workspaces are called similar workspaces. Within the similar workspaces, the GCI values are the same as those of the others. The manipulators which have such a performance similarity are called *similarity manipulators*. Then, the ratios of geometric parameters R_j of all *similarity manipulators* are constant. Any one of the non-dimensional manipulators in the established design space stands for all of its possible *similarity manipulators*. Based on the obtained atlases shown in Figs. 4, 5 and 7–9, one can know the performances of any one of the *similarity manipulators*. For example, if one wants to know the singularity, workspace and GCI performances of a manipulator with $R_1 = 26$ mm, $R_2 = 30$ mm and $r_3 = 16$ mm, one can do that using the atlases and related equations. One should first calculate the parameter D using Eq. (28), e.g., here $D = 24$ mm. Then, with Eq. (29), r_1, r_2 and r_3 can be obtained as $r_1 = 1.08$, $r_2 = 1.25$ and $r_3 = 0.67$. From Fig. 2(b), because $r_1 < r_2$, $r_1 > r_3$ and $r_2 < r_1 + r_3$ the manipulator is located in the sub-region Va. From Fig. 4, one can know all singular loci of the manipulator. Fig. 5 can give information about the singular loci of the manipulator with both the '+−" working mode and the *up-configuration*. The dimensional manipulator also has such singular loci in its workspace. Fig. 7 shows its *usable workspace* shape. From Fig. 8, one knows that the *usable workspace* area of the non-dimensional manipulator is a value between 9.0 and 10.0. The workspace is comparatively small. Then the workspace area for the dimensional manipulator is a value between 216.0 and 240.0 mm. From Fig. 9, one knows that the GCI is near 0.4. All in all, the results shown in Figs. 4, 5 and 7–9 can provide enough information for one to reach the result that the *usable workspace* and GCI performances of the manipulator are comparatively not good.

Because any one of the non-dimensional manipulators in the established design space can represent the performances of all of its possible *similarity manipulators*, the design space is a useful tool for guaranteeing a global comparative result for all manipulators, and also for guaranteeing a global optimum result in the design issue.

10. Conclusions

In this paper, the singularity, workspace and conditioning index of the 5R symmetrical parallel manipulator with a surrounded workspace are investigated systematically in an established design space, in which any one of the non-dimensional manipulators can stand for all of its possible *similarity manipulators* in terms of performances. The analysis shows that

- For manipulators in sub-region IVa where $r_1 + r_3 < r_2$ and $r_1 > r_3$, there is no singularity where B_1PB_2 is completely extended.
- Manipulators in other sub-regions where $r_1 + r_3 > r_2$ have the singularity where B_1PB_2 is completely extended.
- The *usable workspace* presented in Fig. 7 is such a workspace that the manipulator with the "+−" working mode and *up-configuration* can be continuously reached without singularity.
- When r_1 is specified, the *usable workspace* area is inversely proportional to r_3. The manipulator with the largest *usable workspace* is that with $r_3 = 0.0$. Exactly, it is the manipulator with $r_1 = 1.5$, $r_2 = 1.5$ and $r_3 = 0.0$.
- If r_1 is specified, the GCI value is inversely proportional to r_3. The manipulator with the best GCI is in the sub-region where $r_2 > r_1 + r_3$ and $r_1 > r_3$, and $r_3 = 0.0$.
- The singularity, *usable workspace*, and GCI atlases and the results presented here will be different for a manipulator with other working and assembly modes.

The results are very useful for the optimum design of the manipulator with respect to workspace and conditioning index.

The most important result of the paper is the atlases. One important advantage of such an atlas is that it can give designers global and visual information on what kind of manipulator can have good or best performance. Applied in the optimum design of the manipulator, the atlases can be used to obtain an optimum region with a specified workspace and GCI value. The region contains useful information on the geometric parameters. Based on the information, one can select a non-dimensional manipulator directly, or search for a most optimal result in further using one classical searching algorithm. The non-dimensional manipulators in the optimum region are comparative results. They may not be used in some applications because of the small workspace. But they stand for all of their own *similarity manipulators*. Therefore, they are very important for determining a dimensional manipulator for an expected practical workspace. Comparing the desired workspace of a dimensional manipulator with the *good-condition workspace* of its counterpart with non-dimensional parameters, the dimensional factor D can be obtained. The factor is very important for reaching the final design result as shown in the text. The optimum example given in the paper is for showing how the optimum design tool and method work. It could be different if the design specification was changed with respect to a specified application. Anyway, a desired optimum result can finally be reached using the presented atlases.

The design method is useful for getting a global optimum result because of the design space. The process of plotting atlases is time consuming. But the atlases are the things done once and good for ever. When designers want to design a manipulator with respect to an application, what they should do is to compare the atlases and obtain an optimum region. After selecting a non-dimensional manipulator from the region, they can reach the result when the factor D is obtained comparing the desired workspace with the *good-condition workspace*. Therefore, the method is possibly a unified one.

Acknowledgements

This work was supported by the National Natural Science Foundation of China (No. 50505023), and partly by Tsinghua Basic Research Foundation.

The first author wishes to acknowledge the support from the Alexander von Humboldt (AvH) Foundation when he was an AvH Research Fellow at University of Stuttgart in Germany from March 2004 to April 2005.

References

[1] K.M. Lee, D.K. Shah, Part 1: kinematic analysis of a 3-DOF in-parallel actuated manipulator, IEEE Journal of Robotics and Automation 4 (1988) 354–360.

[2] J.-P. Merlet, Direct kinematic and assembly motion parallel manipulators, International Journal of Robotics Research 11 (2) (1992) 150–162.

[3] J.P. Merlet, C.M. Gosselin, N. Mouly, Workspace of planar parallel manipulators, Mechanism and Machine Theory 33 (1–2) (1998) 7–20.

[4] C.M. Gosselin, J. Angeles, Singularity analysis of closed loop kinematic chains, IEEE Transactions on Robotics and Automation 6 (2) (1990) 281–290.

[5] X.-J. Liu, J. Wang, F. Gao, L.-P. Wang, On the analysis of a new spatial three degrees of freedom parallel manipulator, IEEE Transactions on Robotics and Automation 17 (6) (2001) 959–968.

[6] I.A. Bonev, D. Zlatanov, C.M. Gosselin, Singularity analysis of 3-DOF planar parallel mechanisms via screw theory, ASME Journal of Mechanical Design 125 (2003) 573–581.

[7] J.-P. Merlet, Designing a parallel manipulator for a specific workspace, The International Journal of Robotics Research 16 (1997) 545–556.

[8] E. Ottaviano, M. Ceccarelli, Optimal design of CaPaMan (Cassino Parallel Manipulator) with a specified orientation workspace, Robotica 20 (2002) 159–166.

[9] C.M. Gosselin, J. Angeles, The optimum kinematic design of a spherical three degree-of-freedom parallel manipulator, ASME Journal of Mechanisms, Transmissions, and Automation in Design 111 (1989) 202–207.

[10] C.M. Gosselin, The optimum design of robotic manipulators using dexterity indices, Robotics and Autonomous Systems 9 (1992) 213–226.

[11] R.S. Stoughton, T. Arai, A modified Stewart platform manipulator with improved dexterity, IEEE Transactions on Robotics and Automation 9 (2) (1993) 166–173.

[12] J. Ryu, J. Cha, Optimal architecture design of parallel manipulators for best accuracy, in: Proceedings of the 2001 IEEE/RSJ International Conference on Intelligent Robots and Systems, Maui, Hawaii, USA, 2001, pp. 1281–1286.

[13] H.S. Kim, L.-W. Tsai, Design optimization of a Cartesian parallel manipulator, Journal of Mechanical Design 125 (1) (2003) 43–51.

[14] G. Alici, An inverse position analysis of five-bar planar parallel manipulators, Robotica 20 (2002) 195–201.

[15] F. Gao, X. Zhang, Y. Zhao, H. Wang, A physical model of the solution space and the atlases of the reachable workspaces for 2-DOF parallel plane wrists, Mechanism and Machine Theory 31 (2) (1996) 173–184.

[16] J.J. Cervantes-Sánchez, J.C. Hernández-Rodríguez, J.G. Rendón-Sánchez, On the workspace, assembly configurations and singularity curves of the RRRRR-type planar manipulator, Mechanism and Machine Theory 35 (2000) 1117–1139.

[17] F. Gao, X.-J. Liu, W.A. Gruver, Performance evaluation of two-degree-of-freedom planar parallel robots, Mechanism and Machine Theory 33 (6) (1998) 661–668.

[18] F.C. Park, J.W. Kim, Singularity analysis of closed kinematic chains, Journal of Mechanical Design 121 (1999) 32–38.

[19] J.J. Cervantes-Sánchez, J.C. Hernández-Rodríguez, J. Angeles, On the kinematic design of the 5R planar, symmetric manipulator, Mechanism and Machine Theory 36 (2001) 1301–1313.

[20] G. Alici, B. Shirinzadeh, Optimum synthesis of planar parallel manipulators based on kinematic isotropy and force balancing, Robotica 22 (2004) 97–108.

[21] D.C. Tao, A.S. Tall, Analysis of a symmetrical five-bar linkage, Product Engineering 23 (1952) 175–177, 201, 203, 205.

[22] T.W. Lee, F. Freudenstein, Synthesis of geared 5-bar mechanisms for unlimited crank rotations and optimum transmission, Mechanism and Machine Theory 13 (1978) 235–244.

[23] H. Zhou, E.H.M. Cheung, Analysis and optimal synthesis of hybrid five-bar linkages, Mechatronics 11 (2001) 283–300.

[24] X.-J. Liu, J. Wang, F. Gao, Performance atlases of the workspace for planar 3-DOF parallel manipulators, Robotica 18 (5) (2000) 563–568.

[25] G. Strang, Linear Algebra and its Application, Academic Press, New York, 1976.

[26] J.K. Salisbury, J.J. Craig, Articulated hands: force control and kinematic issues, International Journal of Robotics Research 1 (1) (1982) 4–12.

[27] C.A. Klein, B.E. Blaho, Dexterity measures for the design and control of kinematically redundant manipulators, International Journal of Robotics Research 6 (2) (1987) 72–82.

[28] J. Angeles, C. Lopez-Cajun, The dexterity index of serial-type robotic manipulators, ASME Trends and Developments in Mechanisms, Machines and Robotics (1988) 79–84.

[29] C. Gosselin, J. Angeles, The optimum kinematic design of a planar three-degree-of-freedom parallel manipulators, ASME Journal of Mechanisms, Transmissions, Automations. Design 110 (1) (1988) 35–41.

[30] C. Gosselin, J. Angeles, A global performance index for the kinematic optimization of robotic manipulators, Transaction of the ASME. Journal of Mechanical Design 113 (1991) 220–226.

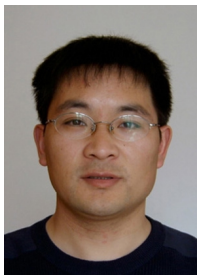

Xin-Jun Liu received the Ph.D. degree in Mechanical Design and Theory from Yanshan University, Qinhuangdao, China, in 1999, the M.S. and B.S. degrees in Machine Design and Manufacture and Mechanics from Northeast Heavy Machinery Institute in 1994 and 1995, respectively.

Currently, he is an Associate Professor in Department of Precision Instruments at Tsinghua University, Beijing, China. From 2000 to 2001, he worked as a Postdoctoral Researcher at Tsinghua University. He was a Visiting Researcher at Seoul National University, Seoul, Korea in 2002–2003. He was an Alexander von Humboldt (AvH) Research Fellow at University of Stuttgart in Germany from 2004 to 2005. He has published over 60 papers in refereed journals and refereed conference proceedings. His research interests include parallel mechanisms, micromanipulators, parallel kinematic machines, and motion simulators.

Dr. Liu received the "Best Youth Paper" Award from "IEEE/ CSS", Beijing Chapter, and the "Excellent Postdoctoral Fellow" Award from Tsinghua University in 2002.

Jinsong Wang received the B.S., M.S. and Ph.D. degrees in mechanical engineering from Tsinghua University, China, in 1986,1988 and 1991, respectively.

He joined Tsinghua University in 1990, and is currently the vice-president of Tsinghua University and a full professor in the school of mechanical engineering. His primary research interests are parallel mechanisms, legged robots, numerical control, machining equipment and green manufacturing.

Dr. Wang is a member of the IEEE and the ASME.

Hao-Jun Zheng received the B.S., M.S. and Ph.D. degrees in mechanical engineering from Tsinghua University, China, in 1993, 1996 and 2000, respectively.

He joined Tsinghua University in 1999, and is currently an Associate Professor in the School of Mechanical Engineering. His research interests are robots, numerical control and machining equipment.